ionization energy, IE, of the radical was found to be 8.25 ± 0.08 eV, eq 10 and 11. Taking $\Delta H_f(t\text{-BuSS}\cdot) = -4.6$ kcal mol^{-1} (Table I) leads to $\Delta H_f(t\text{-BuSS}^+) = 195 \pm 2$ kcal mol^{-1}.

$$\text{RSS}\cdot + e \xrightarrow{\text{IE(10)}} \text{RSS}^+ + 2e \quad (10)$$

$$\text{AE(10)} = \Delta H_f(\text{RSS}^+) - \Delta H_f(\text{RSS}\cdot) = \text{IE(RSS}\cdot) \quad (11)$$

Disulfide Photochemistry. One of the most interesting photochemical properities of dialkyl disulfides is that direct irradiation predominantly cleaves the S–S bond (BDE = 74 ± 2 kcal mol^{-1})[4] even though it is some 20 kcal mol^{-1} stronger than the S–C bond (Table II). By contrast, triplet-sensitized photolysis cleaves the weaker S–C bond.[3,20,21] Presumably, the singlet excited states of dialkyl disulfides are dissociative so that fragmentation to give two alkylthiyl radicals is faster than intersystem crossing to the triplet state. The latter must be lower lying than the singlet since it can be accessed by sensitization using benzophenone, for which the triplet energy (69 kcal mol^{-1})[22] is less than the S–S bond strength (Figure 1).

Summary

The energy required to fragment a series of mixed disulfides (RSS–*t*-Bu) to give RSS· and *t*-Bu$^+$ was found to be independent of the nature of R. Measurements of these appearance energies led to data for the heats of formation of perthiyl radicals, S–C bond dissociation energies in disulfides, and S–S bond dissociation energies for the central bond in tetrasulfides. Thermolysis of di-*tert*-butyl tetrasulfide in the mass spectrometer provided a source of *t*-BuSS· perthiyl radical, allowing measurement of its ionization energy.

(20) Byers, E. W.; Gruen, H.; Giles, H. G.; Schott, H. N.; Kampmeier, J. A. *J. Am. Chem. Soc.* **1972**, *94*, 1016.
(21) Rosenfeld, S. M.; Lawler, R. G.; Ward, H. R. *J. Am. Chem. Soc.* **1972**, *94*, 9255.
(22) Murov, S. L. *Handbook of Photochemistry*; Marcel Dekker: New York, 1973; p 3.

Cyclodextrin Inclusion Complexes of 1-Pyrenebutyrate: The Role of Coinclusion of Amphiphiles

William G. Herkstroeter, Peter A. Martic, Ted R. Evans, and Samir Farid*

Contribution from the Research Laboratories, Eastman Kodak Company, Rochester, New York 14650. *Received October 22, 1985*

Abstract: Several inclusion complexes with various stoichiometries are formed from 1-pyrenebutyrate ion (P) and the different cyclodextrins (α-, β-, and γ-CD). With α- and β-CD, the initially formed 1:1 complexes lead to the formation of 1:2 complexes (P·α_2 and P·β_2). As P can be only partially included in the small cavity of α-CD, the equilibrium constants for the formation of both complexes of α-CD are about an order of magnitude smaller than those of β-CD. For the same reason, P·β_2, to which we assign a "barrel" configuration, is also an order of magnitude more effective than P·α_2 in protecting singlet-excited P against quenching by triethanolamine. We had shown earlier that with γ-CD the 1:1 complex (P·γ) dimerizes to a 2:2 complex (P_2·γ_2), to which we also assigned a barrel configuration. The lack of efficient 1:2 complex formation in this case is attributed to the large size of the "barrel" enclosed by two γ-CD molecules. The extra space next to a single P molecule in such a cavity would have to be filled with water. However, the formation of a 1:2 inclusion complex between P and γ-CD can be induced by the coinclusion of a molecule with a hydrophobic moiety such as sodium hexanesulfonate (X). This replaces the water within the cavity and leads to the formation of P·X·γ_2. This complex provides the highest degree of protection against quenching of excited P in these inclusion complexes.

Cyclodextrins (CD's) are cyclic oligosaccharides that form inclusion complexes with appropriate guest molecules. The smallest of these molecules, α-CD, consists of six glucose units and has a cavity diameter of 5.7 Å. The next higher homologues, β-CD with seven glucose units and γ-CD with eight glucose units, have cavity diameters of 7.8 and 9.5 Å, respectively.[1] Because all hydroxyl groups are on the exterior of these nearly cylindrical molecules, their cavities present hydrophobic environments. It is this property that enables CD's to extract, hold, and protect hydrophobic molecules from aqueous solutions.

The alteration of photophysical properties through CD inclusion is the subject of much current research. Because of its long fluorescence lifetime, we find the pyrene moiety to be an attractive probe for such studies. A number of studies have been based on molecular pyrene, but consistency of results among different investigators is lacking.[2-4] For example, one study of the pyrene/β-CD system reports both 1:1 and 2:2 complexes together with time-dependent shifts ("aging" effects),[2] whereas two other studies report only 1:1 complexes.[3,4] For the weakly interacting combination of pyrene and α-CD, the source of disagreement was whether pyrene or a pyrene dimer undergoes hydrophobic interactions with the exterior surface of α-CD.[3,4] Most likely many of these inconsistencies are traceable to the low solubility limit (1.6×10^{-6} M) of pyrene in water; even at an intended concentration of 5×10^{-7} M in water, excimer fluorescence, attributed to pyrene microcrystals, is observed.[2] As shown recently, unless special precautions are taken in sample preparation, attempted dissolution of pyrene in water even below the solubility limit may lead to microcrystal formation or adherence to glass surfaces, with consequent unreliable solution concentrations of pyrene.[5]

Even with the water-soluble 1-pyrenesulfonate, several investigators report inconsistent results.[3,6,7] We chose to work instead with water-soluble sodium 1-pyrenebutyrate (P), because it has

(1) Szejtli, J. *Starch/Staerke* **1978**, *30*, 427.
(2) Edwards, H. E.; Thomas, J. K. *Carbohydr. Res.* **1978**, *65*, 173.
(3) Kano, K.; Takenoshita, I.; Ogawa, T. *J. Phys. Chem.* **1982**, *86*, 1833.
(4) Yorozu, T.; Hoshina, M.; Imamura, M.; Shizuka, H. *J. Phys. Chem.* **1982**, *86*, 4422.
(5) Patonay, G.; Rollie, M. E.; Warner, I. M. *Anal. Chem.* **1985**, *57*, 569.
(6) Harada, A.; Nozakura, G. *Polym. Bull. (Berlin)* **1982**, *8*, 141.
(7) Kobashi, H.; Takahashi, M.; Muramatsu, Y.; Morita, T. *Bull. Chem. Soc. Jpn.* **1981**, *54*, 2815.

0002-7863/86/1508-3275$01.50/0

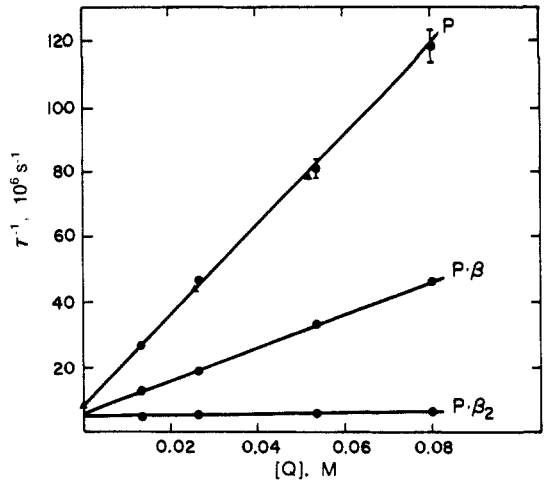

Figure 1. Lifetimes of free and β-CD-complexed P as a function of [Q] at 25 °C. The triangles are from measurements in the absence of β-CD.

a longer singlet lifetime (124 ns for P compared with 65 ns for 1-pyrenesulfonate in water at 25 °C) and is more readily purified.

Recently we showed that in aqueous solution P and γ-CD combine in ratios of 1:1 and 2:2 to yield the inclusion complexes P·γ and its dimer P_2·γ_2.[8] The loss of resolution in the absorption spectrum of the latter and the excimeric fluorescence associated with this species provided the means for determination of the dimerization equilibrium constant. The equilibrium constant for the formation of P·γ and the corresponding thermodynamic data were determined from fluorescence lifetime measurements carried out in the presence of a quencher to enhance the difference between the lifetime of singlet-excited free P and that of the complex P·γ.

This paper describes the use of similar techniques to investigate equilibria involving P and the smaller inclusion hosts β-CD and α-CD. We also studied complex formation of P with γ-CD in the presence of other species that can be coincluded with P in the large cavity of γ-CD. Detailed analysis of the latter system revealed the presence of several different complexes. Such multicomponent systems present an attractive route to control the course of complexation by cyclodextrins.

Results and Discussion

Inclusion Complexes with α- and β-CD. Addition of β-CD to dilute aqueous solutions of P caused a small red shift of ~170 cm^{-1} in the absorption spectrum of P. This effect is similar to that encountered when P and γ-CD combine in a 1:1 complex.[8] These small shifts in absorption suggest that P is in an environment less polar than water, as would be expected when included in a CD cavity. At higher concentrations of P, however, a marked contrast between the effects of β- and γ-CD is observed. With γ-CD, the absorption spectrum of P broadens and excimer fluorescence appears, whereas with β-CD, the sharpness of the absorption spectrum is unaffected and the fluorescence spectrum remains free of an excimer band.

Although we see no P dimer with β-CD, there are, nevertheless, three distinct monomeric pyrene species that can be distinguished by fluorescence lifetime measurements. From first-order plots of the logarithm of fluorescence intensity vs. time, one can determine the number and relative quantities of the components present as a function of [β-CD]. Once corrections have been made for differences in absorption intensities and fluorescence efficiencies, ratios of relative quantities extrapolated to zero time determine equilibrium constants.

In practice, we measured these lifetimes in the presence of triethanolamine [$N(CH_2CH_2OH)_3$, Q], a quencher for singlet-excited pyrene. The purpose of Q was to make the three monomeric pyrene species in the presence of β-CD more amenable to measurement by increasing the lifetime differences between them. Figure 1 shows the lifetime of the three fluorophores as a function of [Q].

(8) Herkstroeter, W. G.; Martic, P. A.; Farid, S. *J. Chem. Soc., Perkin Trans. 2* **1984**, 1453.

Table I. For Both Free and β-CD-Complexed P*,[1] Temperature Dependence of Reaction Constants (k_q)[a] for Quenching by Q and Also of Lifetimes[b] (τ_0) in the Absence of Q

	k_q, M^{-1} s^{-1}			τ_0, ns	
T, °C	P	P·β	P·β_2	P	P·β_2
7	9×10^8	3×10^8	1.6×10^7	133	253
25	1.4×10^9	5.1×10^8	2.7×10^7	124	213
45	2.3×10^9	8.5×10^8	4.6×10^7	116	179

[a] The quenching constants (k_q) were determined from the slopes of the plots of τ^{-1} vs. [Q] as shown in Figure 1. [b] τ_0 is the singlet-excited lifetime in the absence of Q. For free P, the measurements were obtained with no CD added. For P·β_2 the values of τ_0 were obtained by extrapolation of the plots of τ^{-1} vs. [Q] (cf. Figure 1). The corresponding plots for P·β are much steeper. Therefore, extrapolation to determine its τ_0 is of limited accuracy. At 25 °C this is estimated to be 160 ns.

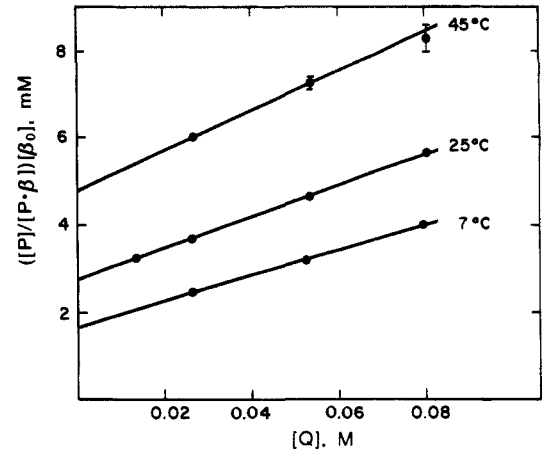

Figure 2. Plots of experimental data according to eq 4 to determine K_A and K_C. [β_0] = 3 mM (7 °C), 2.7 mM (25 and 45 °C).

The dependence of the lifetime of P on [Q] in the absence of CD parallels that of the steepest curve in Figure 1. Accordingly, the species responsible for this curve is assigned to "free" P. the remaining two species must be complexes of P with β-CD. In the plots of the logarithm of fluorescence intensity vs. time, the ratio at zero time of the component with the intermediate quenching rate constant to uncomplexed P increases linearly with increasing equilibrium concentration of β-CD, showing that this species is a 1:1 complex P·β. The ratio of the third component to P·β is also linearly proportional to the equilibrium concentration of β-CD. This third component, the fluorescence lifetime of which varies least with [Q], is thus assigned to a 1:2 complex, P·β_2. The equilibria between P and β-CD are described by eq 1 and 2.

$$P + \beta \overset{K_A}{\rightleftharpoons} P\cdot\beta \quad (1)$$

$$P\cdot\beta + \beta \overset{K_B}{\rightleftharpoons} P\cdot\beta_2 \quad (2)$$

For these three forms of monomeric P, the rate constants for fluorescence quenching by Q are taken from the slopes of the individual plots of Figure 1. Comparing the values of 1.4×10^9, 5.1×10^8, and 2.7×10^7 M^{-1} s^{-1} for P, P·β, and P·β_2, respectively, shows that protection for P increases with the degree of complexation. Table I lists these quenching constants and lifetimes (τ_0) in the absence of Q, measured not only at 25 °C but also at 7 and 45 °C.

By extrapolating the fluorescence decay curves to zero time and also applying corrections for differences in extinction coefficients and quantum yields,[9] we measured the equilibrium ratios [P]/[P·β]

(9) The actual value of [P]/[P·β] is obtained by multiplying the experimentally determined ratio from the decay curves by 0.77; because the absorption spectra of P·β and P·β_2 are quite similar, no correction was applied to the ratio of concentrations of these two species.

Table II. Temperature Effect on the Equilibrium Constants of Complex Formation of β-CD with P and with Q

T, °C	K_A, L mol^{-1} [a]	K_B, L mol^{-1} [b]	K_C, L mol^{-1}
7	600	67	18
25	370	44	13
45	210	27	10

[a] Error margin ±5%, $\Delta H^\circ = -4.9 \pm 0.3$ kcal mol^{-1}, $\Delta S^\circ = -4.7 \pm 1$ cal K^{-1} mol^{-1}. [b] Error margin ±10%, $\Delta H^\circ = -4.4 \pm 0.7$ kcal mol^{-1}, $\Delta S^\circ = -7.4 \pm$ cal K^{-1} mol^{-1}.

and $[P{\cdot}\beta]/P{\cdot}\beta_2]$ at different initial $[\beta]$. Determination of the equilibrium constants requires further corrections for a minor complex formation between Q and β-CD, which decreases free [β-CD] (eq 3). The equilibrium constants K_A, K_B, and K_C were

$$Q + \beta \overset{K_C}{\rightleftharpoons} Q{\cdot}\beta \tag{3}$$

determined from the slopes and intercepts of the linear plots (Figure 2) of the concentration ratios vs. [Q] according to eq 4 and 5. Thermodynamic parameters for the formation of these

$$\frac{[P]}{[P{\cdot}\beta]}[\beta_0] \approx \frac{1}{K_A} + \frac{K_C}{K_A}[Q] \tag{4}$$

$$\frac{[P{\cdot}\beta]}{P{\cdot}\beta_2]}[\beta_0] \approx \frac{1}{K_B} + \frac{K_C}{K_B}[Q] \tag{5}$$

complexes were determined from the measurements at different temperatures (listed in Table II).

Addition of α-CD, the CD with the smallest cavity, to an aqueous solution of P also led to a slight shift in the absorption spectrum (~130 cm^{-1}) comparable to that encountered with β-CD. Also comparable to the results with β-CD was the observation, based on lifetime differences at various [Q], of two separate complexes between P and α-CD, although the second such species is present in small quantities and offers only slightly greater protection than the first against quenching. We applied the same methods described above to determination of complex stoichiometries, equilibrium constants, and quenching constants. The parallel with β-CD extends to the stoichiometries of the complexes whose formation is shown in eq 6 and 7 but not to the

$$P + \alpha \overset{K_D}{\rightleftharpoons} P{\cdot}\alpha \tag{6}$$

$$P{\cdot}\alpha + \alpha \overset{K_E}{\rightleftharpoons} P{\cdot}\alpha_2 \tag{7}$$

magnitude of the equilibrium constants and the quenching constants. At 25 °C we estimate K_D to be ~25 M^{-1} and K_E to be ~3 M^{-1}, whereas the respective quenching constants are 8×10^8 and 3×10^8 M^{-1} s^{-1}. That both equilibrium constants for inclusion in α-CD are about an order of magnitude smaller than the corresponding values with β-CD undoubtedly reflects the poor match in size between guest and host with α-CD.

Coinclusion of Sodium Hexanesulfonate in γ-CD. It is interesting that P forms a 1:2 inclusion complex ($P{\cdot}\beta_2$) with β-CD, whereas with γ-CD such a 1:2 complex is formed inefficiently if at all.[10] The predominant complex containing two γ-CD molecules is the 2:2 complex $P_2{\cdot}\gamma_2$. The reason for such different modes of complexation must be the difference in CD cavity sizes.

We had assigned a "barrel" configuration to the γ-CD dimer in the 2:2 complex.[8] For $P{\cdot}\beta_2$, which most likely also has its β-CD dimer in a "barrel" configuration, CPK models show that the more limited cavity space can accommodate only one P molecule. Inside the γ-CD "barrel", however, the models show a loose fit for a single P molecule. In such a 1:2 complex, the extra space would have to be filled with water molecules, which in turn would render the environment of the hydrophobic pyrene moiety polar and result in strongly diminished stabilization.

If, on the other hand, a second hydrophobic species besides P were present in solution, a relatively stable complex ought to form with one molecule each of P and the second species inside the γ-CD "barrel". To test this hypothesis, we used sodium hexanesulfonate (X) as such an additive. It has the advantage of being water soluble and having a sizeable hydrophobic portion, yet it does not form micelles, which would complicate the analysis. Indeed, addition of X to P and γ-CD decreased the ratio of dimeric to monomeric pyrene complexes. As expected, this change paralleled a decrease in the excimeric fluorescence. Furthermore, when high γ-CD concentrations (≥0.02 M) leave only a negligible quantity of free P, fluorescence lifetime measurements of monomeric pyrene in the presence of Q show two components with distinct lifetimes. The shorter-lived component corresponds to the lifetime of the 1:1 complex P·γ, whereas the other is substantially longer lived and is almost unaffected by [Q]. A_1 and A_2 are designations for the relative quantities of the shorter and longer lived components, respectively; as experimentally measurable quantities, they can be used in ratio form to test various kinetic possibilities. The kinetic data presented below support assignment of the second species to the predicted coinclusion complex $P{\cdot}X{\cdot}\gamma_2$.

Table III. Ratios of the Short- to Long-Lived Components, A_1/A_2, as a Function of the Concentrations (mM) of the Reactants $[\gamma_0]$, $[Q_0]$, and $[X_0]$ at 25 °C[a]

$[\gamma_0]$	$[Q_0]$	$[X_0]$	$[\gamma]$[b]	$[X]$[b]	A_1/A_2
20	128	9.9	7.77	8.57	9.10
20	128	11	7.70	9.53	8.17
20	128	32	6.70	28.2	4.16
20	128	54	5.88	48.3	3.20
20	128	101	4.65	92.4	3.00
20	128	152	3.78	141	3.94
50	128	10.0	21.1	7.03	4.05
50	128	10.2	21.1	7.17	3.83
50	128	32.0	18.3	23.4	1.69
50	128	32.4	18.3	23.7	1.60
50	128	53.8	16.1	40.7	1.17
20	37	10	13.0	7.94	6.20
20	37	29	10.7	23.9	2.70
20	37	50	8.89	42.5	2.08
20	37	150	4.81	13.7	2.16
50	36.8	10	35.0	5.88	2.65
50	36.8	15	33.5	8.98	1.92
50	36.8	25	30.5	15.5	1.31
50	36.8	51	24.7	34.1	0.88
50	36.8	101	17.5	74.9	0.75
50	36.8	201	10.6	166	1.20

[a] $[P_0]$ and [NaOH] were kept constant at 1×10^{-5} and 1×10^{-4} M, respectively. [b] $[\gamma]$ and [X] are the equilibrium concentrations calculated according to eq 11 and 12, respectively, taking $K_5 = 12$ M^{-1} and $K_6 = 20$ M^{-1}.

The possibility that the two components detected by fluorescence decay are P·γ and P·X·γ is readily ruled out. This would have led to a linear increase in the measured ratio (A_2/A_1) with increasing [X], the equilibrium concentration of X. The data in Table III do not fit such a prediction even if we assume that X can be included alone in the CD cavity.

If we now assume that the long-lived species is $P{\cdot}X{\cdot}\gamma_2$, then the question is whether the short-lived species is P·γ alone or a mixture of P·γ and P·X·γ. If it were P·γ alone, the measured ratio A_1/A_2 would correspond to $[P{\cdot}\gamma]/[P{\cdot}X{\cdot}\gamma_2]$ and would be expected to increase linearly with $[X][\gamma]$, where [X] and $[\gamma]$ represent equilibrium concentrations. When put to the test, the fit of the resulting plot to linearity is poor.

On the other hand, if P·X·γ is present and has a fluorescence lifetime similar to that of P·γ, the measured component ratio A_1/A_2 would correspond to $\{[P{\cdot}\gamma] + [P{\cdot}X{\cdot}\gamma]\}/[P{\cdot}X{\cdot}\gamma_2]$. The next question is whether X can be included alone in γ to form X·γ and if so how large the equilibrium constant for such a reaction would

(10) Trace amounts of a longer lived species were detected in the monomeric pyrene fluorescence decay curves. The ratio of this component to P·γ increases slightly but not linearly with [γ]. The exact composition of this minor component, which may represent more than one species, is not clear. It can be estimated, however, that $P{\cdot}\gamma_2$, if at all present, has an equilibrium constant of formation <1 M^{-1}.

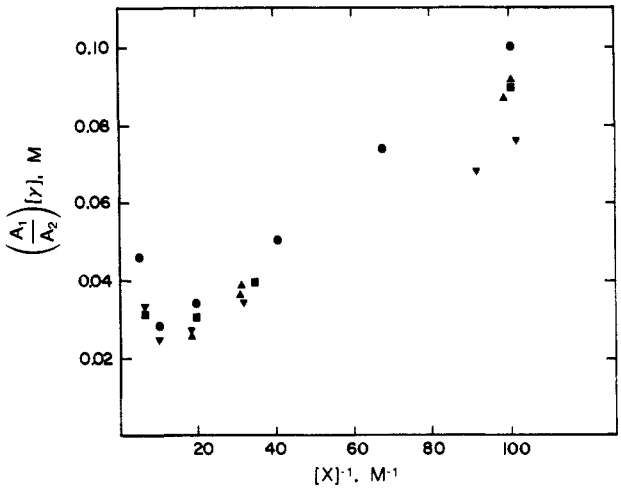

Figure 3. Test of linearity of experimental data plotted according to eq 8 using an assumed K_6 value of 0. The four sets of data points as represented by ▽, △, □, and ○ were derived from the respective four sets of data in Table III in the order listed.

Scheme I

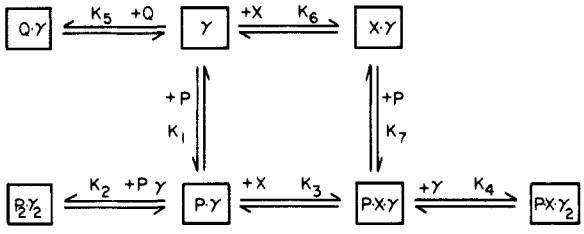

be. To address this point, we consider the overall reaction scheme involving P, γ, Q, and X.

In Scheme I, K_1, K_2, and K_5 had been determined previously and have values at 25 °C of 1.28×10^3, 5.2×10^4, and 12 M^{-1}, respectively.[8] On the basis of this scheme, eq 8 was derived. This

$$\left\{\frac{[P\cdot\gamma] + [P\cdot X\cdot\gamma]}{[P\cdot X\cdot\gamma_2]}\right\}[\gamma] = \frac{1}{K_4} + \frac{1}{K_3K_4}\frac{1}{[X]} \qquad (8)$$

correlates the experimentally measured component ratio A_1/A_2 with $[\gamma]$ and [X]. The latter are the equilibrium concentrations of γ and X, which are lower than the initial concentrations $[\gamma_0]$ and $[X_0]$ owing to equilibria 5 and 6. Because $[\gamma_0]$ is about 3 orders of magnitude higher than $[P_0]$, the fraction of $[\gamma_0]$ involved in complexes with P is negligibly small. It follows that $[\gamma]$ and [X] are given by eq 9 and 10. Accordingly, $[\gamma]$ can be calculated from eq 11 and [X] from eq 12.

$$[\gamma] = [\gamma_0] - [Q\cdot\gamma] - [X\cdot\gamma] \qquad (9)$$

$$[X] = [X_0] - [X\cdot\gamma] \qquad (10)$$

$$K_5K_6[\gamma]^3 + \{K_5K_6([X_0] + [Q_0] - [\gamma_0]) + K_5 + K_6\}[\gamma]^2 + \{1 + K_5[Q_0] + K_6[X_0] - (K_5 + K_6)[\gamma_0]\}[\gamma] - [\gamma_0] = 0 \qquad (11)$$

$$[X] = \frac{[X_0]}{1 + K_6[\gamma]} \qquad (12)$$

On the basis of eq 8, a linear relationship is expected for a plot of the component ratio A_1/A_2 multiplied by $[\gamma]$ vs. $[X]^{-1}$. The equilibrium concentrations $[\gamma]$ and [X] depend on the values of K_5 and K_6 according to eq 11 and 12. As mentioned above, K_5 was determined previously to be 12 M^{-1}. Calculations based on $K_6 = 0$ gave a poor fit for a linear relationship, as shown in Figure 3. The linear fits were improved as we assumed higher values for K_6. Reasonably good correlation coefficients were obtained from plots based on K_6 values between 15 and 20 M^{-1}. As an example, Figure 4 shows the data calculated for $K_6 = 20$ M^{-1}. Table IV gives the corresponding K_3 and K_4 obtained from the slope and intercept of such least-squares-fitted straight lines.

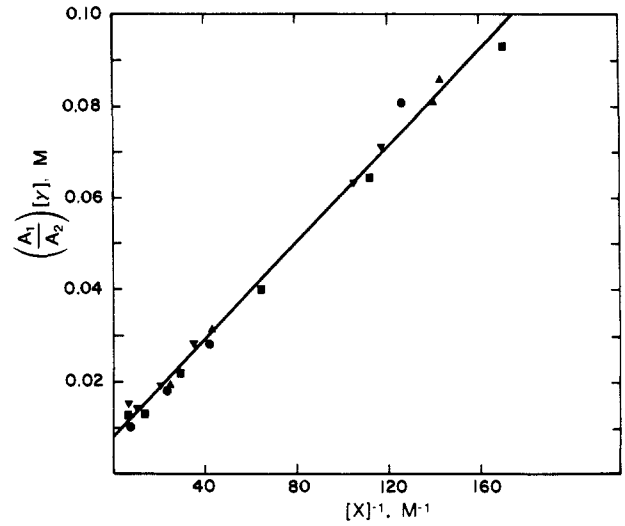

Figure 4. Test of linearity of experimental data plotted according to eq 8 using an assumed K_6 value of 20 M^{-1}. The four sets of data points as represented by ▽, △, □, and ○ were derived from the respective four sets of data in Table III in the order listed. Slope = 5.3×10^{-4} M^2; intercept = 7.7×10^{-3} M.

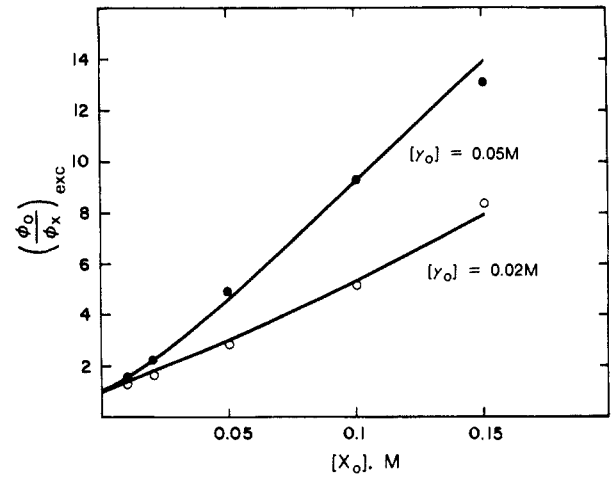

Figure 5. Plots of the ratios of excimer fluorescence in the absence (ϕ_0) and the presence of (ϕ_x) of X as a function of $[X_0]$ and at two different $[\gamma_0]$; $[P_0]$ was constant at 1.04×10^{-5} M. The points are from experimental measurements; the curves are calculated from eq 13 using the equilibrium constants determined from Figure 4 ($K_6 = 20$ M^{-1}, $K_3 = 14.6$ M^{-1}, $K_4 = 130$ M^{-1}.

Table IV. Calculated Equilibrium Constants K_3 and K_4 for Assumed Values of K_6

assumed value K_6, M^{-1}	corresponding Values, M^{-1}		correlation coeff
	K_3	K_4	
15	15.7	112	0.9972
18	15.0	123	0.9970
20	14.6	130	0.9966

Additional support for this overall equilibrium scheme and our analysis of it was obtained by measuring the decrease in $[P_2\cdot\gamma_2]$ with increasing $[X_0]$. For these experiments no quencher was needed. $[P_2\cdot\gamma_2]$ is given by eq 13, where $a = [1 + (1/$

$$[P_2\cdot\gamma_2] = \left\{\left[(a + b[X])^2 + \frac{[P_0]}{2}\right]^{1/2} - (a + b[X])\right\}^2 \qquad (13)$$

$K_1[\gamma])]/4(K_2^{1/2})$ and $b = (K_3 + K_3K_4[\gamma])/4K_2^{1/2}$. In the absence of Q, $[\gamma]$ is obtained from the following quadratic equation and [X] by substituting for $[\gamma]$ in eq 12:

$$K_6[\gamma]^2 + (1 + K_6[X_0] - K_6[\gamma_0])[\gamma] - [\gamma_0] = 0 \qquad (14)$$

Table V. Fluorescence Lifetimes of Free and Complexed P[a,b]

	P								
T, °C	H_2O	1-propanol	cyclohexane	P·α	P·β	P·γ	P·α_2	P·β_2	P·X·γ_2
7	133	208	263			155		253	
25	124	200	258	(132)	(160)	147	(145)	213	230
45	118	192	253			138		179	

[a] All complexes were in water as solvent. [b] Values in parentheses are estimates from limited data (with α-CD) or associated with larger error (with β-CD).

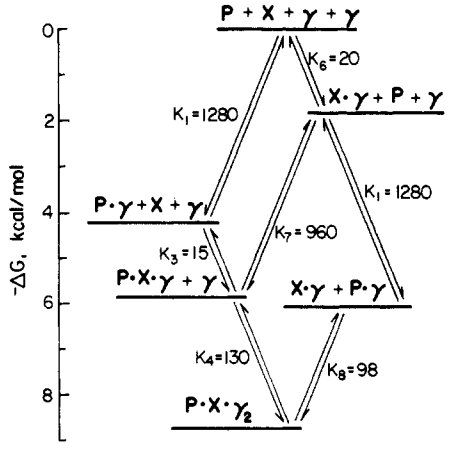

Figure 6. Overall equilibrium scheme at 25 °C involving P, X, and γ calibrated in terms of ΔG relative to uncomplexed starting reagents P, X, and γ-CD.

The intensity of the excimeric emission was used as a measure for $[P_2{\cdot}\gamma_2]$. It is convenient to evaluate the data in the form of $(\phi_0/\phi_x)_{exc}$, where ϕ_0 and ϕ_x are the excimer intensities in the absence and in the presence of X, respectively. A plot of this ratio vs. $[X_0]$ at two values of $[\gamma_0]$ is shown in Figure 5. The curves in this figure are calculated according to eq 13 for $K_6 = 20$ M^{-1} together with the corresponding values of K_3 and K_4 from Table IV.[11] The fact that the same set of equilibrium constants correlate well with two different and independent experimental measurements provides strong support for the validity of the proposed scheme and the determination of the equilibrium constants.

From the equilibrium constants mentioned above, the free energy changes ($-\Delta G$) associated with the different equilibria are calculated (cf. Figure 6). The values for K_7 and K_8 are derived from their relationship to other equilibrium constants according to eq 15 and 16. According to Figure 6, the free energy change

$$K_1K_3 = K_6K_7 \quad (15)$$

$$K_4K_7 = K_1K_8 \quad (16)$$

associated with bringing together a molecule of P, a molecule of X, and two molecules of γ-CD to form P·X·γ_2 is 8.7 kcal/mol.

Coinclusion of species such as X, which shifts the course of complex formation from the dimeric pyrene complex $P_2{\cdot}\gamma_2$ to the monomeric P·X·γ_2, offers an attractive method for forming certain inclusion complexes that might otherwise not take place.

The concentration of P in all of these experiments was between 1×10^{-5} and 2×10^{-5} M. To ensure complete dissolution of P, a five-to-tenfold excess of NaOH was added to each solution. This low concentration ($\leq 1 \times 10^{-4}$ M) of base has no apparent effect on the experimentally determined equilibrium constants.

The influence of higher base concentrations was investigated for the case of P and γ-CD. No significant changes in spectra were detectable when the NaOH concentration was increased to 1×10^{-3} M, but 1×10^{-2} M base led to a small decrease in the concentration of the dimeric complex $P_2{\cdot}\gamma_2$. Further increases in NaOH concentrations brought about substantial decreases in the ratio of $P_2{\cdot}\gamma_2$ to the monomeric components P·γ and P. These observations are traceable to substantial reductions in K_1 and K_2. Reduced CD complex formation above pH 12 has also been reported for other systems.[12]

Ionic strength independent of pH can also have an effect on equilibria involving P and the CD's. For example, NaCl shifts the ratio of $P_2{\cdot}\gamma_2$ to P·γ in the opposite direction than NaOH, if the concentration is high enough. In a solution with starting concentrations of P and γ-CD of 1×10^{-5} and 0.02 M, respectively, 0.16 M NaCl effects only a small shift in this ratio, whereas 10 times as much salt leads to a distinct shift in favor of the dimer. Quantitative measurements of pH and ionic strength effects on such equilibria are still in progress and will be reported in a subsequent paper.

Table VI. Quenching Rate Constants for Free and Complexed P[a]

fluorophore	$(k_q)_Q$, M^{-1} s^{-1}	$(k_q)_{O_2}$,[b] M^{-1} s^{-1}
P	1.4×10^9	9.4×10^9
P·α	$\sim 8 \times 10^8$	
P·β	5.1×10^8	4.6×10^9
P·γ	2.6×10^8	4.4×10^9
P·α_2	$\sim 3 \times 10^8$	
P·β_2	2.7×10^7	1.8×10^9
P·X·γ_2	$<3 \times 10^6$ [c]	4×10^8

[a] All measurements were taken at 25 °C. [b] These values were obtained from measurements of lifetimes in oxygen-saturated aqueous solutions where $[O_2] = 1.3 \times 10^{-3}$ M. [c] The change in the lifetime of P·X·γ_2 with increasing [Q] is within the range of experimental error of our lifetime measurements. The k_q value listed is an upper limit, but the actual rate constant could be much lower.

Lifetimes and Quenching Rate Constants. A noteworthy effect of P complexation with CD's with no quenchers present is the lengthening of the fluorescence lifetime. At 25 °C the lifetime of free P^{*1} is 124 ns, but it increases to 130–160 ns inside the various 1:1 complexes. However, in the complexes with two β- or γ-CD molecules, P·β_2 and P·X·γ_2, there is a considerably larger increase to 210–230 ns. We attribute these increases in τ_0 to the less polar environment of CD cavities. This assignment is based on comparisons of uncomplexed P^{*1} lifetimes in water, 1-propanol, and cyclohexane; the lifetime is longer in a less polar medium. Table V lists these fluorescence lifetimes at 25 °C together with some measured at 7 and 45 °C.

The τ_0 values for P·β_2 are substantially more temperature dependent than those for free P whether in water, 1-propanol, or cyclohexane. What this may mean for P·β_2 is that the average separation between the two β-CD molecules increases as the vibrational freedom increases with temperature. Any intrusion of water into the space between the two CD molecules would increase the environmental polarity of included P and lead to shortened lifetimes.

The level of protection of P from the aqueous environment as reflected by the increase in τ_0' parallels the decrease in the reaction constants for quenching the excited host. As described above, quenching data are obtained from the variation in lifetime as a function of concentration according to eq 17 (cf., for example, Figure 1). Free P^{*1} is quenched by Q with a k_q of 1.4×10^9

$$\frac{1}{\tau} = \frac{1}{\tau_0} + k_q[Q] \quad (17)$$

M^{-1} s^{-1}. The corresponding reaction constants for all 1:1 complexes

(11) Of the three sets of values for the equilibrium constants in Table IV, all of which gave good fits with the data from lifetime measurements, the set corresponding to $K_6 = 20$ M^{-1} gave the best fit with excimer intensity data.

(12) Cox, G. S.; Turro, N. J.; Yang, N. C.; Chen, T.-J. *J. Am. Chem. Soc.* **1984**, *106*, 422.

as well as the poorly protected P·α_2 fall in the range (3–5) × 10^8 M^{-1} s^{-1}. Sharp drops in the rate constant for quenching are encountered for P·β_2 and P·X·γ_2. Of all complexes considered, the latter species protects included P best; its k_q is, in fact, too small to be determined by the technique used here. All rate constants for quenching of P*[1] both outside and inside its various inclusion complexes are included in Table VI, along with the rate constants for quenching by molecular oxygen (O_2), an alternative quencher of much smaller molecular dimensions.

The high degree of protection against quenching and the hydrophobic environment of P in the complexes with two β- or γ-CD molecules strongly supports the proposed "barrel" configuration of these complexes. Placing P inside a barrel-like enclosure made up with two CD molecules should offer protection superior to that possible with 1:1 complexes. Shown are schematic representations of such barrel complexes. Because the barrels have openings at

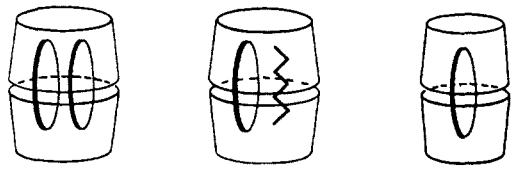

$P_2 \cdot \gamma_2$ $P \cdot X \cdot \gamma_2$ $P \cdot \beta_2$

each end and possibly each midsection, one might expect these complexes to be more vulnerable to quenching by O_2 than by Q, as they in fact are.

The P·α_2 complex deserves special comment. CPK models show that α-CD can fit only partially over one end of P. In a 1:2 complex, a second α-CD could go to the other end of the P molecule, but the poor fit does not permit the two α-CD molecules to close around the midsection of the included P to form a "barrel". Instead, the best these smallest CD molecules can do is to put P into a "sandwich". Our experimental measurements of τ_0 and k_q for P·α_2 (Tables V and VI, respectively) give values that are comparable to those obtained for other 1:1 complexes but not for complexes involving either two β-CD or two γ-CD molecules.

Our systematic study of inclusion complexes of the pyrene derivative P with the cyclodextrins illustrates the importance of the size match between guest and host. Working with a water-soluble pyrene derivative eliminated complications associated with the low solubility limit of molecular pyrene in water and permitted quantitative analysis of the equilibrium constants of complexation as well as unambiguous determination of both the complex stoichiometries and the extent of protection against excited-state quenching.

Coinclusion of different hydrophobic speices by CD's offers some exciting possibilities. In the example we have reported on, X, by means of coinclusion, shifts the course of complexation between P and γ-CD away from the otherwise preferred path to a new species in which P and γ-CD combine in a different molecular ratio. Furthermore, among the various complexes that P forms with each of the CD's, this coinclusion complex provides the best protection for P against excited-state quenching.

Experimental Section

We prepared P by dissolving 1-pyrenebutyric acid (Kodak reagent grade) in 0.5 M sodium hydroxide solution, adding saturated sodium chloride solution to precipitate P, filtering, and recrystallizing the precipitate from ethanol. α-, β-, and γ-CD (Sigma Chemical Co.), Q (Kodak reagent grade), and X (Kodak reagent grade) were used as received.

All absorption spectra were measured on a Hitachi Perkin-Elmer Model 320 spectrophotometer equipped with temperature-controlled cell holders. Fluorescence spectra and fluorescence lifetimes were measured with a Spex Fluorolog II spectrofluorimeter and a Photochemical Research Associates fluorescence-lifetime apparatus, respectively. Fluorescence-lifetime analysis of two- and three-component systems was by the method of least-squares iterative reconvolution using the Marquardt algorithm.[13,14]

Summary

The inclusion complexes that P forms in aqueous solution with each of α-, β-, and γ-CD are compared. We have reported details of the equilibria leading to complex formation and have measured rate constants for fluorescence quenching of P, both free in solution and in its various complexes.

P is best isolated by complexes containing two molecules of β-CD or γ-CD. We propose that each pair of CD molecules forms a barrel-like enclosure around included P. Although one molecule of P fills the β-CD "barrel", two P molecules are required for the larger γ-CD "barrel". Coinclusion of species such as X,[15] which shifts the course of complex formation from the dimeric pyrene complex $P_2 \cdot \gamma_2$ to the monomeric P·X·γ_2, offers an attractive method forming certain inclusion complexes that might otherwise not take place.

Acknowledgment. We are grateful to Prof. F. C. DeSchryver and Dr. N. Boens of the University of Leuven, Belgium, for providing us with a copy of their program for analysis of the fluorescence decay data. We also thank Dr. R. L. Reeves of the Kodak Research Laboratories for valuable discussions.

(13) O'Connor, D. V.; Ware, W. R.; Andre, J. C. *J. Phys. Chem.* **1979**, *83*, 1333.

(14) Boens, N.; Van den Zegel, M.; De Schryver, F. C. *Chem. Phys. Lett.* **1984**, *111*, 340.

(15) After completion of this manuscript, a paper appeared by Hashimoto and Thomas[16] dealing with coinclusion of pyrene and amphiphiles by β-CD.

(16) Hashimoto, S.; Thomas, J. K. *J. Am. Chem. Soc.* **1985**, *107*, 4655.